Journal of Applied Polymer Science

The effect of mass transfer resistance and nonuniform initial solvent concentration on permeation through polymer membranes

John M. Zielinski [1], Sacide Alsoy Altinkaya [2]
[1]Intertek Chemicals and Pharmaceuticals, Allentown Pennsylvania
[2]Department of Chemical Engineering, Izmir Institute of Technology, Izmir, Turkey
Correspondence to: J. M. Zielinski (E-mail: john.zielinski@intertek.com)

ABSTRACT: A numerical simulation model has been developed which enables one to examine the effects of surface mass transfer resistance on the evaluation of permeation (P^*), diffusion (D), and solubility (S) coefficients from unsteady-state mass transfer experiments as well as the transmission rate. A complementary analytical expression has been developed which validates the numerical model and facilitates the evaluation of the concentration dependence of P^*, D, and S from sequential step-change experiments, under experimental conditions when the surface mass transfer resistance can be neglected. © 2017 Wiley Periodicals, Inc. J. Appl. Polym. Sci. **2018**, *135*, 46126.

KEYWORDS: membranes; separation techniques; theory and modeling

Received 10 July 2017; accepted 20 November 2017
DOI: 10.1002/app.46126

INTRODUCTION

Transmission rates of solvents and moisture through polymer films are often measured to evaluate the barrier properties of the polymers and to evaluate the extent of protection offered by the polymers in defending the components they encapsulate. For example, nitrile gloves are used to safeguard hands from exposure to chemicals, while silicone potting material is commonly employed to shield electronic components from exposure to moisture. Although steady-state transmission rates are typically measured, and reported, the time at which exposure to chemicals or moisture occurs is dictated by the diffusion coefficient (D) rather than by the transmission rate or permeability.

Permeation coefficients (P^*) reflect the amount of penetration of a substance through a solid over a period of time. Permeation involves the molecular diffusion of the penetrant molecules from high to low concentration and is directly related to the chemical affinity of the permeant with the solid. The nature of the penetrant-solid interaction is represented through the slope of the isotherm, otherwise termed the solubility coefficient (S), which reflects the amount of the penetrant contained within the solid as a function of pressure at a fixed temperature.

The equations of Crank[1] and Frisch[2] have been widely applied to examine the time lag in diffusion/permeation experiments. Time-lag solutions[1–4] typically applied to evaluate P^*, D, and S coefficients assume that the initial concentration of solvent is uniform throughout the membrane. Moreso, the membrane is commonly assumed to contain no solvent initially. Experimental studies are commonly conducted in the same manner, that is, the membrane is dried out before each solvent exposure in order to start with an initial zero solvent concentration profile across the sample. Although this practice provides known initial and boundary conditions for the experiment, which correspond to the typical time lag solution, it limits the rate at which experimental data can be acquired.

Performing measurements in a stepwise fashion, as is done in gravimetric sorption experimentation,[5] is a much more expedient practice. For example, for a water vapor transmission test, a typical sequence could be to initially dry out the membrane with a nitrogen purge gas or with vacuum. One side of the membrane could then be exposed to 5% relative humidity (RH) while the other side is maintained at 0% RH (step 1). Once a steady-state transmission rate is achieved, the gas phase on the upstream side of the membrane could be increased from 5% RH to 10% RH, while the downstream side is maintained at 0% RH (step 2). Although this is a more expedient experimental practice, the resulting transmission rate profile is very different than when the membrane initially contains no solvent. In addition, the typical time lag solution[1,2] is only applicable for step 1, since initially there is no solvent within the polymer film. The time lag model is not applicable for step 2 and must be corrected, since there is an initial solvent gradient across the membrane at the end of step 1 and, consequently, at the start of step 2 and all subsequent permeation experiments.

The second critical assumption utilized in the time-lag solution is the absence of mass transfer resistance in exiting the polymer

membrane and entering the carrier gas. Although this simplification enables the development of straightforward analytical expressions, the surface mass transfer resistance has been found to be critical in understanding, and representing, the drying of polymer solutions and similarly must be considered in establishing experimental conditions that are suitable for determining permeation, diffusion, and solubility coefficients in membrane transport experiments.

Cairncross,[6,7] Hadj Romdhane *et al.*,[8] Alsoy and Duda,[9] among others, have shown that understanding mass transfer resistance in the gas phase is a key aspect in accurately modeling the drying of polymer solutions for practical drying schemes. In these analyses, two mass transfer resistances were considered: (1) the diffusion of solvent within the polymer matrix and (2) the mass transfer resistance at the surface of the membrane where the solvent evaporates from the polymer solution and is swept into the convective stream of the sweep gas. The drying models have been useful in predicting the effect of experimental conditions, for example, temperature, carrier gas velocity, etc., on the solvent transport process and have been used to define conditions which optimize the rate of devolatilization. The analysis of polymer film drying with a concentration- and temperature-dependent diffusion coefficient,[10] is easily amenable to represent solvent permeation in a polymer membrane.

Permeation through polymers has been investigated analytically by modified time-lag analyses[1–4,11] and with various diffusion models,[12] within finite volume systems[13–15] and at various experimental conditions.[16–20] Application of time-lag analysis[21–29] has been applied to extract diffusion information along with permeation data and both dual sorption[30–32] and free volume theories[33–35] have been proposed to understand the transport mechanism within polymer membranes.

Although permeation through polymer membranes has been extensively examined and modeled, none of the previous analyses considered the effect of a mass transfer zone (MTZ) on the exiting side of the membrane during a transient transport experiment. This is surprising since drying of polymer membranes and solvent permeation are analogous transport processes and the effect of an MTZ on steady-state processes has been examined.[36,37] As one develops experimental capabilities to measure transient, solvent permeation rates, understanding the effect of a mass transfer resistance on the resulting permeation, diffusion, and solubility coefficients should be known, as should be the experimental conditions at which the MTZ is eliminated.

Unfortunately, incorporation of a gas-phase MTZ in the permeation analysis significantly complicates the development of an analytical solution. To address the MTZ analysis we have opted instead to develop a numerical solution of the transport equations, since further complications such as nonlinear concentration profiles, concentration-dependent diffusion coefficients, multicomponent transport, etc., can be readily accommodated and are envisioned as the subject of future investigations.

In this work, we present a numerical simulation model which enables one to examine the effects of surface mass transfer resistance on the transmission rate and on the evaluation of P^*, D, and S coefficients from unsteady-state mass transfer experiments. A complementary analytical expression has been developed which validates the numerical model, and facilitates the evaluation of the concentration dependence of P^*, D, and S from sequential step-change experiments, under experimental conditions when the surface mass transfer resistance can be neglected. This modified time lag expression assumes a linear concentration gradient across the membrane at the beginning and end of each transient experiment. To the best of our knowledge, this work is the first which discusses the combined effect of nonuniform initial concentration in the membrane and surface mass transfer resistance on the transient permeation curves.

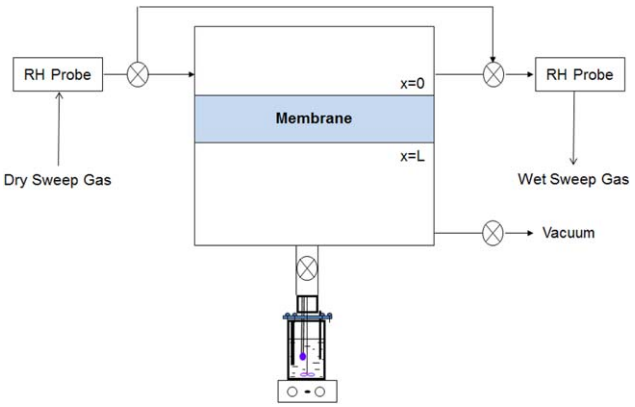

Figure 1. Schematic of the experimental apparatus on which the permeation analyses developed in this work are based. [Color figure can be viewed at wileyonlinelibrary.com]

EXPERIMENTAL

Development of Numerical Simulation Model

A schematic of the experimental apparatus, on which the permeation models developed in this work are based, is provided in Figure 1. This set-up is similar to that used by Zhang[36] to study vapor permeation through composite supported liquid membranes. The solvent flask is maintained at a temperature at or below the temperature of the membrane and therefore is capable of generating conditions up to full vapor saturation. Although the solvent can be any liquid, the extent to which the vapor phase is saturated on the $x = L$ side of the membrane can be considered as the RH (% RH), which is a term generally limited to discussions of water vapor.

Since an initial vacuum can be drawn on the solvent-flask side of the membrane initially, one need not consider a mass transfer resistance in exposing this side of the membrane to the solvent vapor. However, as in the case of drying a polymer solution with a purge gas, the low concentration (downstream) side of the membrane may have a mass transfer resistance in the zone between the polymer surface and the bulk gas phase. The initial and final concentration profiles envisioned for this scenario are depicted in Figure 2.

Here the dotted line indicates the initial condition in the membrane prior to the start of the experiment and the solid line represents the final profile once steady-state has been achieved. C_{2p} and C_{1p} represent the solvent concentration in

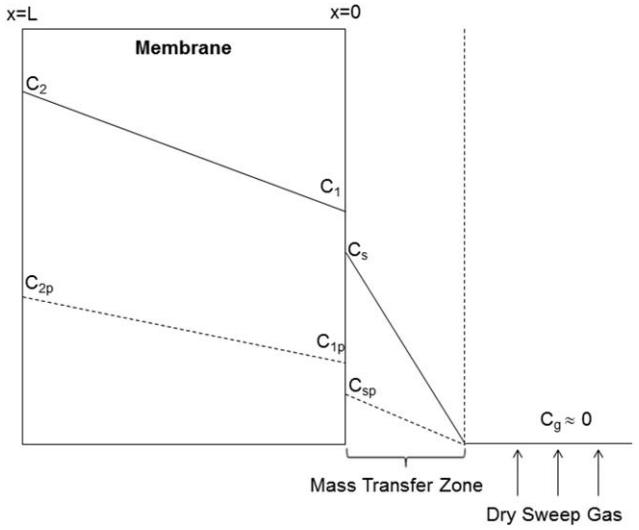

Figure 2. Schematic of concentration profiles assumed for development of the general numerical permeation model when a mass transfer zone exists.

the polymer phase on the upstream and downstream sides of the membrane at the end of the previous step, which is the initial condition prior to the start of the current step. For the case when the polymer membrane is initially dried, C_{1p} and C_{2p} are equal to zero and the initial profile in the membrane is flat. C_2 and C_1 represent the solvent concentration in the polymer phase on the upstream and downstream sides of the membrane after steady-state has been achieved in the current experimental step.

If a dry carrier gas is swept sufficiently quickly across the downstream side of the membrane, the bulk solvent concentration in the gas phase can be assumed to be approximately zero ($C_g \approx 0$). However, depending on the flow characteristics within the system, a MTZ can exist. The solvent concentration in the polymer phase can be assumed to be in equilibrium with the partial pressure of solvent just outside of the polymer film on the downstream side of the membrane. This can be mathematically represented as:

$$C_1 = S \times P_{1S} \tag{1}$$

Here, P_{1S} is the partial pressure of solvent just outside of the polymer film on the downstream side of the membrane and S is a solubility (or partition) coefficient. If one assumes ideal gas behavior, eq. (1) can be written in terms of the gas-phase solvent concentration, namely

$$C_1 = \mathrm{SRT} \times C_S \tag{2}$$

The transport rate across the MTZ is governed by a mass transfer coefficient (k_m) that is characteristic of the solvent, the system geometry, and experimental conditions. This coefficient can be evaluated by performing experiments with no polymer membrane present in the system. A linear driving force model is typically used to describe the transmission rate across the MTZ.

When a permeation experiment is performed such that the step change in the upstream membrane surface concentration is small, the diffusion and solubility coefficients can be assumed to be approximately constant for the duration of the experimental step. In this case, the basic transport equation that describes transport through the polymer membrane is

$$\frac{\partial C}{\partial t} = D\frac{\partial^2 C}{\partial x^2} \tag{3}$$

which is Fick's second law of diffusion. In the scenario portrayed in Figure 2, eq. (3) is subject to the following initial and boundary conditions:

Initial condition ($t = 0$):

$$C_o(x) = f(x) = C_{1p} - [C_{1p} - C_{2p}]\frac{x}{L} \tag{4}$$

Boundary condition 1 ($t > 0$, $x = L$):

$$C = C_2 \tag{5}$$

Boundary condition 2 ($t > 0$, $x = 0$):

$$D\left(\frac{\partial C}{\partial x}\right)_{x=0} = k_m(C_S - C_g) = k_m C_S = \frac{k_m C_1}{\mathrm{SRT}} \tag{6}$$

Here, the solvent concentration in the bulk gas phase (C_g) is assumed to be zero and C_S is represented by eq. (2).

To facilitate programming of the numerical simulation, these equations were recast into dimensionless variables using the following definitions:

$$x^* = \frac{x}{L}; \quad t^* = \frac{Dt}{L^2}; \quad C^* = \frac{C - C_2}{C_2} \tag{7}$$

Substitution of these variables into eqs. (3) through (6) yields

$$\frac{\partial C^*}{\partial t^*} = \frac{\partial^2 C^*}{\partial x^{*2}} \tag{8}$$

This dimensionless form of Fick's law is subject to the following conditions:

Initial condition ($t^* = 0$):

$$C^* = C_o^* = \frac{C_{1p}}{C_2} - \left[\frac{C_{1p} - C_{2p}}{C_2}\right]x^* - 1 \tag{9}$$

Boundary condition 1 ($t^* > 0$, $x^* = 1$):

$$C^* = 0 \tag{10}$$

Boundary condition 2 ($t^* > 0$, $x^* = 0$):

$$\left(\frac{\partial C^*}{\partial x^*}\right)_{x^*=0} = \left[\frac{k_m L}{D}\right]\left[\frac{1}{\mathrm{SRT}}\right][1 + C^*|_{x^*=0}] = \left[\frac{\mathrm{Bi}}{\mathrm{SRT}}\right][1 + C_1^*] \tag{11}$$

Here, the ratio of $k_m L$ to D is referred to as the Biot number, which reflects the relative importance of the mass transport process in the gas phase above the membrane to that within the polymer matrix. In addition, C_1^* is the dimensionless concentration on the downstream side of the membrane ($x^* = 0$) evaluated from the definition provided in eq. (7).

Although the mathematical analysis of the permeation process is written here in terms of surface concentrations, permeation, diffusion, and solubility coefficients are experimentally evaluated by measuring the transmission rate (or flux) and by evaluating the total amount of material transmitted through the membrane in a given period of time (Q_t). Q_t can be evaluated from the developed equations by summing the flux at the polymer-gas phase interface ($x = 0$) over time using either the dimensional or dimensionless variables, since:

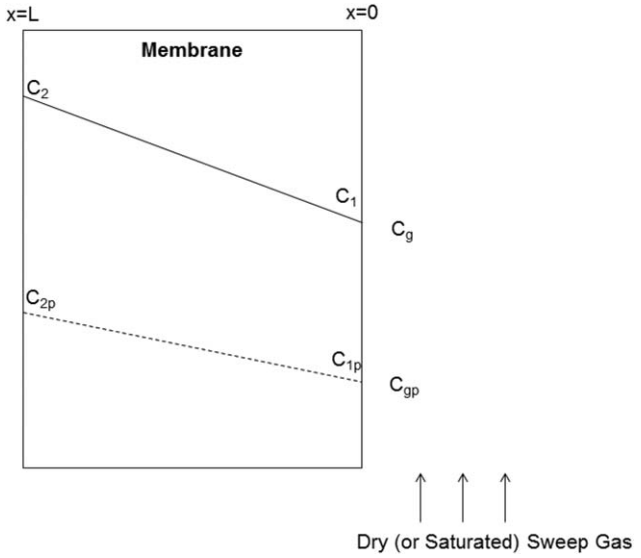

Figure 3. Schematic of concentration profiles assumed for development of the general analytical permeation model when no mass transfer zone exists.

$$Q_t = \int_0^t D\left(\frac{\partial C}{\partial x}\right)_{x=0} dt \quad = \quad LC_2 \int_0^{t^*} \left(\frac{\partial C^*}{\partial x^*}\right)_{x^*=0} dt^* \qquad (12)$$

Thus, by defining D, L, k_m and the surface concentrations, numerical simulations can be performed to predict Q_t as a function of t for a series of experimental conditions.

Development of Analytical Model

To develop a general analytical expression to analyze permeation, the initial and steady-state concentration profiles depicted in Figure 3 are envisioned. In this case, the sweep gas flow is presumed to step from an initial concentration of C_{gp} to a final concentration of C_g. In addition, the system conditions are presumed to have been set so that there is no MTZ at the downstream face of the polymer membrane.

In this scenario, one could imagine that the %RH at $x = L$ is 10% while at $x = 0$ the %RH in the gas phase is maintained at 5% at $t < 0$. There is, therefore, a linear concentration gradient within the film initially. At $t \geq 0$, assume that the %RH is bumped to 25% at $x = L$ and is increased to 10% at $x = 0$. At all times during the course of this experiment the surface concentrations of the polymer will be held constant, but they will be different at $x = 0$ and $x = L$.

Although the concentration profile within the polymer film initially ($t < 0$) is linear, and the surface concentrations are held constant at $x = 0$ and $x = L$, the concentration profile within the film will not be linear at all times during the course of the experiment. The concentration profile will only become linear once steady-state is reached. In addition, there will continue to be non-zero fluxes at $x = 0$ and $x = L$ at steady-state due to the presence of the concentration gradient. Only for the case of the classical two-sided diffusion experiment,[1] where both surfaces of the polymer membrane are held at the same %RH, will a no flux condition be achieved. Under those conditions, the concentration profile within the polymer will be become flat ($dC/dx = 0$) after equilibrium is achieved.

If the carrier gas is a dry sweep gas, the values of C_{gp} and C_g would both be equal to zero. However, for the case of water transmission into a laboratory atmosphere, there may be measurable %RH in the room which would better be represented by a finite water vapor concentration in the gas phase above the membrane. Consequently, the objective here is to develop an analytical expression that can be used to describe both scenarios.

The solutions of many commonly encountered diffusion situations have been worked out by Crank.[1] The case under consideration in Figure 3 is no exception and is described as diffusion in a plane sheet with constant surface concentrations and with an initial solvent concentration distribution. The expression for the solvent concentration as a function of position and time is given as:

$$\begin{aligned} C = C_1 + [C_2 - C_1]\frac{x}{L} + \frac{2}{\pi}\sum_{n=1}^{\infty}\left[\frac{C_2\cos n\pi - C_1}{n}\right]\sin\left(\frac{n\pi x}{L}\right) \\ \times\exp\left[\frac{-Dn^2\pi^2 t}{L^2}\right] + \frac{2}{L}\sum_{n=1}^{\infty}\sin\left(\frac{n\pi x}{L}\right) \\ \times\exp\left[\frac{-Dn^2\pi^2 t}{L^2}\right]\int_0^L f(x)\sin\left(\frac{n\pi x}{L}\right)dx \end{aligned} \qquad (13)$$

As is stated by Crank, however, in the cases of most common occurrence the initial concentration profile across the membrane, $f(x)$, is either zero or constant so that the integral in eq. (13) is readily evaluated. To form a more generally applicable solution, the initial concentration profile is assumed here to be linear and written as eq. (4). Substitution of eq. (4) into eq. (13) and evaluation of the integral leads to the following expression for the solvent concentration profile:

$$\begin{aligned} C = C_1 + [C_2 - C_1]\frac{x}{L} + \frac{2}{\pi}\sum_{n=1}^{\infty}\left[\frac{C_2\cos n\pi - C_1}{n}\right]\sin\left(\frac{n\pi x}{L}\right) \\ \times\exp\left[\frac{-Dn^2\pi^2 t}{L^2}\right] + \frac{2}{L}\sum_{n=1}^{\infty}\frac{L}{n\pi}\left[C_{1p} - C_{2p}(-1)^n\right] \\ \times\sin\left(\frac{n\pi x}{L}\right)\exp\left[\frac{-Dn^2\pi^2 t}{L^2}\right] \end{aligned} \qquad (14)$$

The transmission rate, J, through the membrane is experimentally evaluated at the exit of the membrane ($x = 0$) and is given by:

$$\begin{aligned} J_{x=0} = \frac{D[C_2 - C_1]}{L} + \frac{2D}{L}\sum_{n=1}^{\infty}[C_2(-1)^n - C_1]\exp\left[\frac{-Dn^2\pi^2 t}{L^2}\right] \\ + \frac{2D}{L}\sum_{n=1}^{\infty}\left[C_{1p} - C_{2p}(-1)^n\right]\exp\left[\frac{-Dn^2\pi^2 t}{L^2}\right] \end{aligned} \qquad (15)$$

The steady-state transmission rate that is commonly reported is evaluated by measuring the amount of a gas or vapor that passes through a membrane and from knowledge of the sample area exposed to the gas/vapor during the experiment once the system has attained steady-state. The transmission rate is a measure of the flux of gas through the membrane and as such has units of gas/vapor quantity transmitted per area per time. For moisture this rate is referred to as the water vapor transmission rate, but this quantity is nothing more than a flux, which is evaluated by dividing the rate of mass transfer (quantity transmitted per time) by the cross-sectional area of the sample.

The total amount of solvent transmitted across the membrane at any time (Q_t) can be evaluated by integrating eq. (15) over time. The resulting expression is:

$$Q_t = \frac{D[C_2 - C_1]\,t}{L} + \frac{2L}{\pi^2}\sum_{n=1}^{\infty}\left[\frac{C_2(-1)^n - C_1}{n^2}\right]\left[1 - \exp\left[\frac{-Dn^2\pi^2 t}{L^2}\right]\right] + \frac{2L}{\pi^2}\sum_{n=1}^{\infty}\left[\frac{C_{1p} - C_{2p}(-1)^n}{n^2}\right]\left[1 - \exp\left[\frac{-Dn^2\pi^2 t}{L^2}\right]\right] \quad (16)$$

At long times, the permeation process reaches a time-independent transmission rate which, for water, is reported as the water vapor transmission rate. The comparable expression for the steady-state total amount of material transmitted (Q_∞) is developed by examining the long-time behavior of eq. (16). This expression is simply:

$$Q_\infty = \frac{D[C_2 - C_1]\,t}{L} + L\left[\frac{(C_{1p} - C_1)}{3} + \frac{(C_{2p} - C_2)}{6}\right] \quad (17)$$

The transmission rate ($J_{x\,=\,0}$) is not an inherent material property since different sample thicknesses yield different values of $J_{x\,=\,0}$ for the same material. Typically, permeation coefficients are evaluated from the transmission rate data since permeation coefficients reflect the inherent steady-state transmission characteristics of a solvent through a membrane. Permeation coefficients, however, are often functions of temperature and concentration. The permeation coefficient (P^*) can be evaluated from the experimental steady-state transmission rate, $J_{x\,=\,0}(t\to\infty)$, the membrane thickness, and the driving force pressure, since

$$P^* = \frac{J_{x=0}(t \to \infty)\times L}{\Delta P} \quad (18)$$

Here, L is the sample thickness and ΔP is the differential pressure driving force across the membrane. Thus, once a permeation coefficient is known for a polymer-solvent pair, the steady-state transmission rate can be evaluated from knowledge of the applied driving force pressures and the thickness of the membrane.

The analysis performed by Dayes[26] and the measurement scheme developed and popularized by Barrer[27–29] revealed that the diffusion coefficient can be determined from the time lag (t_{LAG}). The time lag is defined as the point intersected when the long-term transmission rate curve is extrapolated back to the time axis.[1–4] It has been suggested that the permeation experiment should be conducted for at least three lag times to achieve steady-state and provide a region of data suitable for extrapolation.[3]

The time lag can be defined from eq. (17) by setting Q_∞ to zero and rearranging the equation to solve for D, namely

$$D = \frac{-L^2}{6t_{\mathrm{LAG}}}\left[\frac{2(C_{1p} - C_1) + (C_{2p} - C_2)}{(C_2 - C_1)}\right] \quad (19)$$

Crank[1] suggests that steady-state is achieved once a value of 0.45 is achieved for the grouping Dt/L^2, which is commonly referred to as the dimensionless time [see eq. (7)], whereas Shah[3] indicates that the permeation profile truly becomes linear after three time lags have been exceeded in the permeation process. Once P^* and D are known, the solubility coefficient (S) can be evaluated from the well-known relationship

$$P^* = D \times S \quad (20)$$

The value of S indicates the affinity between the solvent and the polymer. For example, the solubility coefficient for water vapor will be larger for a hydrophilic material than for a hydrophobic one. Equation (20) also reveals that the permeation rate of a vapor through a material can be increased either by increasing the diffusion rate or by increasing its solubility in the polymer.

Comparison of Numerical and Analytical Solutions

The equations for the numerical solution are expected to yield the same results as those from the analytical solution only when there is no MTZ in the gas phase. This occurs when the mass transfer coefficient is set very high and, as a result, the Biot number is high. This means that the resistance to mass transfer is due to diffusion in the polymer phase rather than due to gas-phase transport from the downstream face of the membrane to the bulk gas phase. In essence, the bulk gas phase extends to the face of the membrane since there is no MTZ and the surface concentration at $x = 0$ remains constant with time. This condition will be established by the parameters selected in the upcoming comparisons.

For the case when an MTZ exists, the modeling of the experiment needs to be performed numerically. The mass transfer coefficient (k_m) can be evaluated from experiments without the membrane present and then used in the numerical analysis to evaluate P^*, D, and S from transmission rate data.

Case 1. As an initial test for the analytical and numerical models, the case of diffusion in a plane sheet with constant surface concentrations and with a uniform, flat initial solvent concentration profile, $C(x) = C_o$ = constant, is considered. A flat profile can either be zero or a finite value, but in either case the initial surface concentrations C_{1p} and C_{2p}, as defined in eq. (4), are equal. In addition, the surface concentration on the downstream side of the membrane (C_1) is maintained at a value of zero, despite the fact that C_{1p}, the concentration at that face of the membrane from the previous step, may not initially be zero.

The test parameters used are defined in Table I and a comparison of the results from the analytical and numerical simulations is provided in Figure 4. Here, the total amount of material transmitted is presented in dimensionless form, that is, $Q_t^* = Q_t/LC_2$, and is plotted as a function of the dimensionless time, $t^* = Dt/L^2$. This was done to provide a simplified visual comparison of the three steps. As a reminder, the Biot number is set to a high value (>1000) in order to eliminate the presence of an MTZ in the numerical solution. There is a difference in curvature of the resulting Q_t^* versus time profiles that is caused by the presence or absence of solvent in the membrane initially. The numerical and analytical results both reflect this difference in the Q_t^* profiles and are found to be in excellent agreement.

For the condition when the membrane is initially at zero solvent concentration and the concentration at the face through which the diffusing substance emerges is maintained at zero, eq. (17) reduces to

Table I. Parameters used in Comparison of Numerical and Analytical Models (Case 1)

Step	$C_o(x) = C_{1p} = C_{2p}$ (g/cm^3)	C_1 (g/cm^3)	C_2 (g/cm^3)	D (cm^2/s)	L (cm)
1	0	0	9.468×10^{-4}	5×10^{-9}	0.005
2	1×10^{-4}	0	9.468×10^{-4}	5×10^{-9}	0.005
3	5×10^{-4}	0	9.468×10^{-4}	5×10^{-9}	0.005
4	1×10^{-3}	0	9.468×10^{-4}	5×10^{-9}	0.005

$$Q_\infty = \frac{DC_2}{L}\left[t - \frac{L^2}{6D}\right] \tag{21}$$

which is in agreement with Crank's solution[1] and provides the time lag permeation solution typically employed.[1,2] For a flat initial profile, $C(x) = C_o$, with the downstream side of the membrane maintained at zero solvent concentration at times greater than zero, the steady-state total amount of material transmitted is given as

$$Q_\infty = \frac{DC_2 t}{L} + \frac{L}{6}\left[3C_o - C_2\right] \tag{22}$$

Case 2. As a second test for the analytical and numerical models, the case of diffusion in a plane sheet with constant surface concentrations and with a linear initial solvent concentration profile, $C(x) = f(x)$, is considered. In addition, the surface concentration on the downstream side of the membrane (C_1) is maintained at a value of zero. Experimentally this may be the most relevant case, since it allows one to start experimentation with a dry membrane, $C(x) = 0$, attain a linear concentration profile once steady-state is achieved and then step the upstream surface concentration to a higher value to monitor the response of the system. In this fashion one need not dry out the membrane between experiments in order to evaluate the permeation, diffusion and solubility coefficients. In addition, performing experiments in a stepwise fashion, as described and as performed in traditional gravimetric sorption experiments, provides a better representation of the concentration dependence of the P^*, D, and S coefficients.

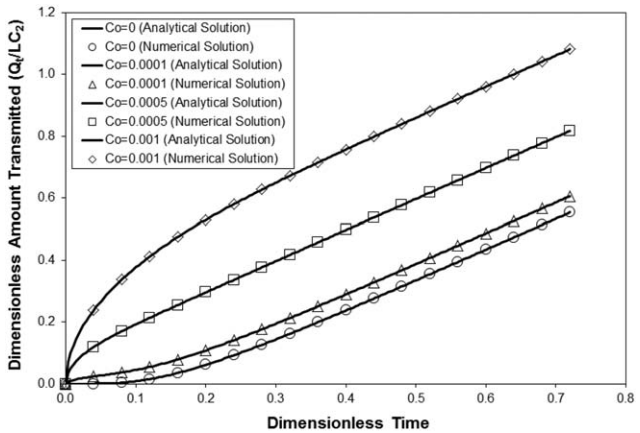

Figure 4. Comparison of analytical and numerical model results for the case of a flat initial concentration profile, that is, $C_o(x) = C_{1p} = C_{2p}$, and when the Biot number and the mass transfer coefficient, k_m, are high (case 1). The parameters used in the models are provided in Table I. Concentrations are given in units of g/cm^3.

The test parameters used are defined in Table II and a comparison of the results from the analytical and numerical simulations is provided in Figure 5. Once again, the Biot number is set to a high value (>1000) in order to eliminate the presence of an MTZ in the numerical solution. These modeling results indicate that experimentally evaluating the time lag is more easily accomplished in step 1, when the linear profile is zero, than in steps 2 and 3 when a finite, linear concentration profile already exists. The conclusion, however, is the same as in case 1 in that the results from the analytical and numerical solutions are in excellent agreement. The results also reveal that care needs to be taken experimentally, to make the concentration steps large enough to be readily measurable.

An initial linear concentration profile can either be flat or have different concentration values on either face of the membrane as defined by the initial surface concentrations C_{1p} and C_{2p} [see eq. (4)]. For the case when the downstream side of the membrane is maintained at a value of zero ($C_{1p} = C_1 = 0$) the resulting expression for Q_∞ is

$$Q_\infty = \frac{DC_2 t}{L} + \frac{L}{6}\left[C_{2p} - C_2\right] \tag{23}$$

This expression is the most useful if stepwise permeation experiments are performed under conditions where there is no MTZ and the downstream surface concentration is maintained at zero.

It is worth noting here that although the membrane thickness (L) can be assumed to be constant for a single experiment in which a step change in the upstream membrane surface concentration is small, the increase in membrane thickness due to swelling should be evaluated (and used in the analysis) based on the solubility and concentration gradient evaluated in the previous step experiment.

Case 3. Since the numerical solution has been shown to match the analytical results accurately, the next set of conditions to be examined is the effect of the MTZ on the permeation process. In this simulation, the initial condition is assumed to be the simplest case of a flat, initial profile of zero solvent concentration, that is, $C_o(x) = 0$. The concentration on the upstream side of the membrane is maintained at the same constant value, only the mass transfer coefficient (k_m) and, consequently, the Biot number is varied. The simulation results are provided in Figure 6 and clearly show that there is a tremendous effect on the resulting permeation curves due to the resistance offered by the MTZ. For the case of a high Biot number, SRT/Bi = 0, the numerical solution matches the results from the analytical solution.

Table II. Parameters used in Comparison of Numerical and Analytical Models (Case 2)

Step	C_{1p} (g/cm^3)	C_{2p} (g/cm^3)	C_1 (g/cm^3)	C_2 (g/cm^3)	D (cm^2/s)	L (cm)
1	0	0	0	0.1	5×10^{-9}	0.005
2	0	0.1	0	0.2	5×10^{-9}	0.005
3	0	0.2	0	0.3	5×10^{-9}	0.005

The effect of the MTZ on the transmission curves shown in Figure 6 is visually apparent. There is, however, nothing obvious in the transmission curves that would indicate that an MTZ exits. Qualitatively, the results from the case of SRT/Bi equals 0 and 0.5 (seen in Figure 6) are similar in that a time lag can be measured and a steady-state transmission rate is achieved at long times. If these were experimental data, however, one could not by visual inspection determine whether an MTZ existed. In addition, one could apply the typical time lag expression, eq. (21), to evaluate P^*, D, and S from either set of data, however, the values obtained would be dramatically different and only for the case of SRT/Bi is equal to zero would they be correct.

For the example provided, that is, SRT/Bi equals 0.5, the MTZ causes up to a 100% error on the diffusion coefficient, an error of 400% on the solubility coefficient and approximately an order of magnitude error in the permeation coefficient if one assumes no MTZ is present. It is critical, therefore, to understand the characteristics of one's experimental set-up and operating conditions. Accurate values of P^*, D, and S can only be evaluated by either assuring that no MTZ exists or by evaluating the mass transfer coefficient for the solvent in the system at the operating conditions and performing the corresponding analysis appropriately.

The difference in the amount of solvent transmitted through the membrane is also reflected in the change in solvent concentration on the downstream surface of the membrane. For the case of a high Biot number, the surface concentration is equal to zero when the concentration of solvent in the sweep gas is zero. The effect of the MTZ on the solvent concentration at the downstream side of the polymer membrane is shown in Figure 7 for two consecutive experimental steps, which are delineated in the caption. Clearly, the solvent concentration at the downstream face of the membrane changes with time.

Case 4. The final analysis is performed to examine the experimentally relevant case of three consecutive permeation experiments in which the upstream membrane concentration is set and the flux is monitored until a steady-state transmission rate is achieved. In the first step (step 1), the membrane contains no solvent, that is, $C_o(x) = 0$, and the upstream surface concentration is set to $C_2 = 0.1$ g/cm^3. The transmission rate is followed until steady-state is achieved at which point there is a steady-state concentration profile across the membrane. A second permeation step (step 2) is then initiated in which the upstream membrane surface concentration is stepped to $C_2 = 0.2$ g/cm^3 and again, the flux is monitored until a new steady-state transmission rate is achieved. Finally, after this new steady-state is achieved there is a different concentration gradient in the membrane than after step 2. The final step (step 3) is made by increasing the upstream membrane concentration to $C_2 = 0.3$ g/cm^3 and following the transmission rate until a final steady-state transmission rate is achieved.

For this analysis three conditions for the MTZ are considered: (1) a high value of the Biot number is set (SRT/Bi = 0), so there is no MTZ, (2) an intermediate value of the Biot number is set (SRT/Bi = 0.5), so the diffusion resistance through the membrane and the MTZ are comparable, and (3) a low value of the Biot number is set (SRT/Bi = 5.0), so the effect of the MTZ is pronounced.

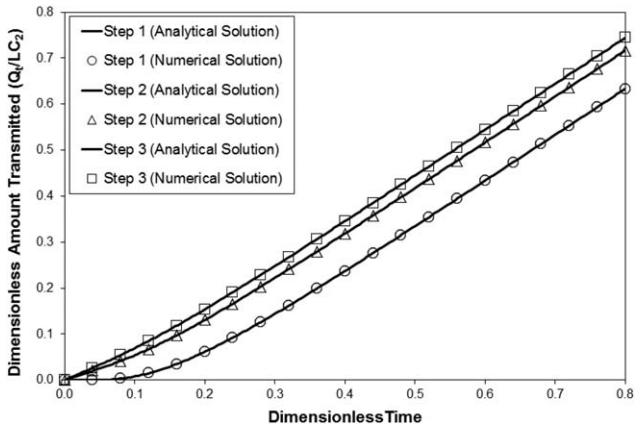

Figure 5. Comparison of analytical and numerical model results for the case of an initial linear concentration profile, that is, $C_o(x) = C_{1p} - [C_{1p} - C_{2p}]x/L$, and when the Biot number and the mass transfer coefficient, k_m, are high (case 2). The parameters used in the models are provided in Table II. Concentrations are given in units of g/cm^3.

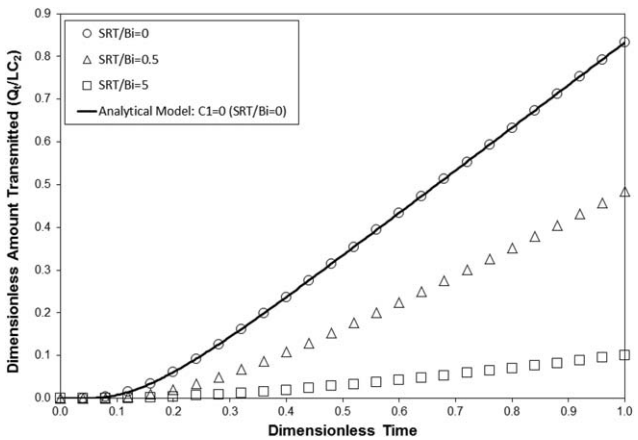

Figure 6. Effect of the mass transfer zone on the permeation process (case 3). As the Biot number increases, the influence of the mass transfer zone decreases. When the Biot number is very large (>1000) the numerical and analytical solutions yield the same results.

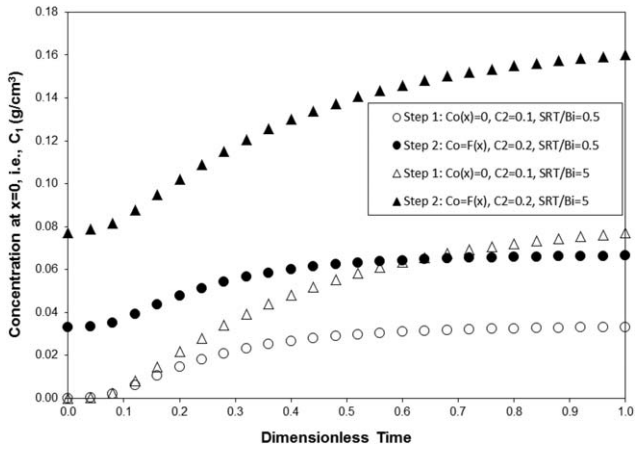

Figure 7. Effect of the mass transfer zone on the solvent concentration at the downstream side of the polymer membrane (case 3). Concentrations are given in units of g/cm^3.

The results of these simulations are provided in Figures 8–10. The axes are purposely scaled the same in these figures to highlight the effect of the MTZ. Clearly, if the flow characteristics for the experimental apparatus allow for appreciable gas phase resistance, the transmission rate measured will not reflect the inherent mass transfer characteristics of the membrane but rather a lumped resistance due to contributions from the membrane as well as the testing conditions.

For the case of a high value of the Biot number, analytical solutions have been developed from which one can evaluate concentration dependence of the transmission rate, P^*, D, and S from each of the experimental steps, that is, eqs. (20) and (23). For the remaining cases in which an MTZ is present, no analytical solution exists. For these cases, the mass transfer coefficient

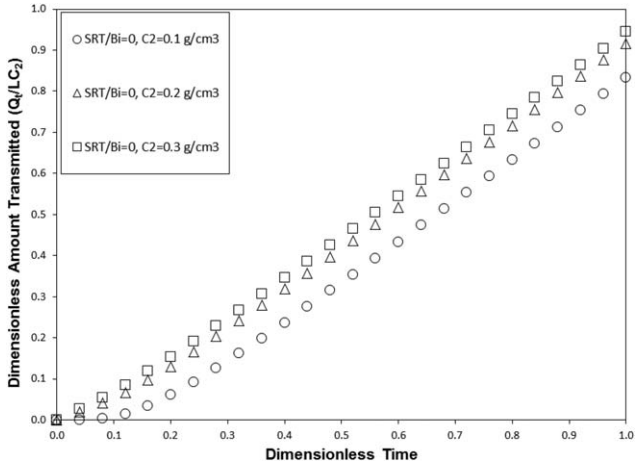

Figure 8. Case 4 simulation results for three consecutive permeation steps for a high value of the Biot number (SRT/Bi = 0). In the first step, the membrane contains no solvent, that is, $C_o(x) = 0$, and the upstream surface concentration is set to $C_2 = 0.1$ g/cm^3. After steady-state is achieved there is a concentration gradient in the membrane and the upstream concentration is increased to $C_2 = 0.2$ g/cm^3. Likewise, after steady-state is achieved there is a concentration gradient in the membrane and the upstream concentration is increased further to $C_2 = 0.3$ g/cm^3.

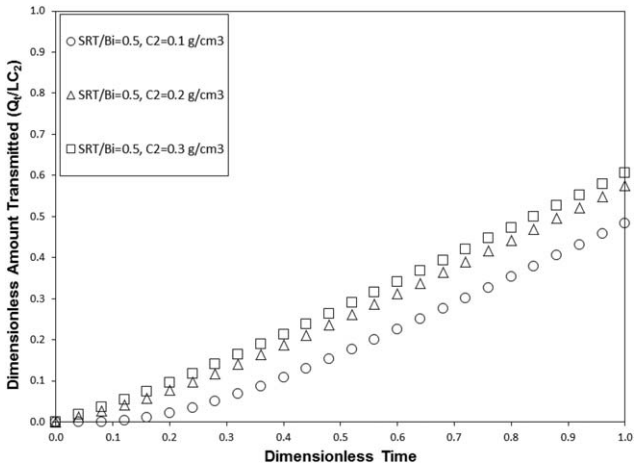

Figure 9. Case 4 simulation results for three consecutive permeation steps for an intermediate value of the Biot number (SRT/Bi = 0.5). In the first step, the membrane contains no solvent, that is, $C_o(x) = 0$, and the upstream surface concentration is set to $C_2 = 0.1$ g/cm^3. After steady-state is achieved there is a concentration gradient in the membrane and the upstream concentration is increased to $C_2 = 0.2$ g/cm^3. Likewise, after steady-state is achieved there is a concentration gradient in the membrane and the upstream concentration is increased further to $C_2 = 0.3$ g/cm^3.

must be assessed from separate experiments and the P^*, D, and S coefficients can be evaluated by numerical regression analysis. In general, however, it is probably better to avoid using an MTZ in an analysis and to define experimental conditions where the MTZ is eliminated.

CONCLUSIONS

In this work a numerical simulation model has been developed which enables one to examine the effects of surface mass

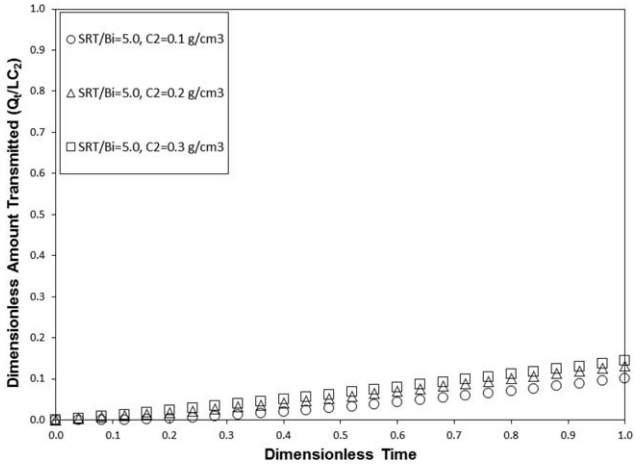

Figure 10. Case 4 simulation results for three consecutive permeation steps for a low value of the Biot number (SRT/Bi = 5.0). In the first step, the membrane contains no solvent, that is, $C_o(x) = 0$, and the upstream surface concentration is set to $C_2 = 0.1$ g/cm^3. After steady-state is achieved there is a concentration gradient in the membrane and the upstream concentration is increased to $C_2 = 0.2$ g/cm^3. Likewise, after steady-state is achieved there is a concentration gradient in the membrane and the upstream concentration is increased further to $C_2 = 0.3$ g/cm^3.

transfer resistance on the evaluation of P^*, D, and S coefficients from unsteady-state mass transfer experiments. The model has been validated by the development of a complementary analytical expression, which was used to compare results at conditions when the surface mass transfer resistance in the numerical simulation could be neglected, that is, at conditions of high Biot number. Modifications of the numerical model can be made readily to examine further complications such as nonlinear concentration profiles, concentration-dependent diffusion coefficients, and multicomponent transport.

The numerical solution reveals the importance of evaluating whether or not a gas-phase mass transfer resistance exists in an experimental unit at the conditions being used, since the transient breakthrough curve of Q_t versus time is qualitatively the same whether or not an MTZ exists. If the typical time lag model commonly employed [eq. (21)] is applied to experimental data collected at conditions in which an MTZ exists, the resulting P^*, D, and S coefficients will be erroneous. For the case SRT/Bi equals 0.5, the MTZ causes up to a 100% error on the diffusion coefficient, an error of 400% on the solubility coefficient and approximately an order of magnitude error in the permeation coefficient if one assumes no MTZ is present.

Lastly, the analytical model developed here has been shown to complement and validate the numerical simulation. The analytical solution explicitly considers a nonzero and nonuniform concentration gradient at the beginning of a permeation experiment under experimental conditions when the surface mass transfer resistance can be neglected. Application of this analytical solution allows for a faster evaluation of the concentration dependence of P^*, D, and S, since sequential step-change experiments can be performed, that is, the membrane does not need to be dried out prior to each successive transient permeation step, as is commonly performed. For this experimental protocol, the concentration step size needs to be sufficiently large in order to accurately discern the time lag in the permeation process. To the best of our knowledge, this work is the first which discusses the combined effect of nonuniform initial concentration in the membrane and surface mass transfer resistance on the transient permeation curves.

REFERENCES

1. Crank, J. The Mathematics of Diffusion, 2nd ed.; Clarendon Press: Oxford, UK, **1975**.
2. Frisch, H. L. *J. Phys. Chem.* **1957**, *61*, 93.
3. Shah, J. C. *Int. J. Pharm.* **1993**, *90*, 161.
4. Taveira, P.; Mendes, A.; Costa, C. *J. Membr. Sci.* **2003**, *221*, 123.
5. Vrentas, J. S.; Duda, J. L.; Ni, Y. C. *J. Polym. Sci. Part B: Polym. Phys.* **1977**, *15*, 2039.
6. Cairncross, R. A.; Durning, C. *AIChE J.* **1996**, *42*, 2415.
7. Cairncross, R.; Jeyadev, S.; Dunham, R.; Evans, K.; Francis, L.; Scriven, L. *J. Appl. Polym. Sci.* **1995**, *58*, 1279.
8. Hadj Romdhane, I.; Price, P. E.; Miller, C. A.; Benson, P. T.; Wang, S. *Ind. Eng. Chem. Res.* **2001**, *40*, 3065.
9. Alsoy, S.; Duda, J. L. *Dry. Technol.* **1998**, *16*, 15.
10. Zielinski, J. M.; Duda, J. L. In Polymer Devolatilization; Marcel Dekker, Inc.: New York, NY, **1996**.
11. Paul, D. R.; DiBenedetto, A. T. *J. Polym. Sci. Part C: Polym. Symp.* **2007**, *10*, 17.
12. Al-Qasas, N.; Thibault, J.; Kruczek, B. *J. Membr. Sci.* **2016**, *511*, 119.
13. Pasternak, R. A.; Schimscheimer, J. F.; Heller, J. *J. Polym. Sci. Part A-2: Polym. Phys.* **1970**, *8*, 467.
14. Barrie, J. A.; Spencer, H. G.; Quig, A. *J. Chem. Soc. Faraday Trans. 1* **1975**, *71*, 2459.
15. Rodrigo Correa, C.; Klein, A. *Polym. Test.* **1990**, *9*, 271.
16. Pasternak, R. A.; Christensen, M. V.; Heller, J. *Macromolecules* **1970**, *3*, 366.
17. Schult, K. A.; Paul, D. R. *J. Appl. Polym. Sci.* **1996**, *61*, 1865.
18. Sebok, B.; Schulke, M.; Reti, F.; Kiss, G. *Polym. Test.* **2016**, *49*, 66.
19. Al-Qasas, N.; Kruczek, B.; Thibault, J. *J. Membr. Sci.* **2014**, *460*, 25.
20. Al-Qasas, N.; Kruczek, B.; Thibault, J. *J. Fluid Flow Heat Mass Transfer* **2014**, *1*, 57.
21. Bhatia, D.; Vieth, W. *J. Membr. Sci.* **1980**, *6*, 351.
22. Zhang, Y. K.; Kocherginsky, N. M. *J. Membr. Sci.* **2003**, *225*, 105.
23. Paul, D. R. *J. Polym. Sci. Part A-2: Polym. Phys.* **1969**, *7*, 1811.
24. Al-Ismaily, M.; Wijmans, J. G.; Kruczek, B. *J. Membr. Sci.* **2012**, *423*, 165.
25. Wu, H.; Al-Qasas, N.; Kruczek, B.; Thibault, J. *J. Fluid Flow Heat Mass Transfer* **2015**, *2*, 14.
26. Dayes, H. *Proc. R. Soc. London Ser. A* **1920**, *97*, 296.
27. Barrer, R. M. Diffusion in and Through Solids; Cambridge University Press: Cambridge, UK, **1951**.
28. Barrer, R. M.; Grove, D. M. *Trans. Faraday Soc.* **1951**, *47*, 837.
29. Barrer, R. M.; Barrie, J. A. *Proc. R. Soc. London Ser. A* **1952**, *213*, 250.
30. Paul, D. R.; Koros, W. J. *J. Polym. Sci. Polym. Phys. Ed.* **1976**, *14*, 675.
31. Toi, K.; Saito, K.; Suganuma, Y.; Ito, T.; Ikemoto, I. *J. Appl. Polym. Sci.* **1992**, *46*, 1939.
32. Guo, J.; Barbari, T. A. *Macromolecules* **2008**, *41*, 238.
33. Vrentas, J. S.; Duda, J. L. *J. Polym. Sci. Polym. Phys. Ed.* **1977**, *15*, 403.
34. Vrentas, J. S.; Duda, J. L. *J. Polym. Sci. Polym. Phys. Ed.* **1977**, *15*, 417.
35. Vrentas, J. S.; Vrentas, C. M. *J. Appl. Polym. Sci.* **1999**, *71*, 1431.
36. Zhang, L.-Z. *Sep. Sci. Technol.* **2006**, *41*, 3517.
37. Berry, M.; Taylor, C.; King, W.; Chew, Y.; Wenk, J. *Water* **2017**, *9*, 452.